JOURNAL OF VIROLOGY, Nov. 2009, p. 11356–11366 Vol. 83, No. 21
0022-538X/09/$12.00 doi:10.1128/JVI.02677-08

Identification of RNA Helicase A as a New Host Factor in the Replication Cycle of Foot-and-Mouth Disease Virus▽†

Paul Lawrence and Elizabeth Rieder*

Foreign Animal Disease Research Unit, United States Department of Agriculture, Agricultural Research Service, Plum Island Animal Disease Center, Greenport, New York 11944

Received 30 December 2008/Accepted 18 July 2009

Foot-and-mouth disease virus (FMDV), as with other RNA viruses, recruits various host cell factors to assist in the translation and replication of the virus genome. In this study, we investigated the role of RNA helicase A (RHA) in the life cycle of FMDV. Immunofluorescent microscopy (IFM) showed a change in the subcellular distribution of RHA from the nucleus to the cytoplasm in FMDV-infected cells as infection progressed. Unlike nuclear RHA, the RHA detected in the cytoplasm reacted with an antibody that recognizes only the nonmethylated form of RHA. In contrast to alterations in the subcellular distribution of nuclear factors observed during infection with the related cardioviruses, cytoplasmic accumulation of RHA did not require the activity of the FMDV leader protein. Using IFM, we have found cytoplasmic RHA in proximity to the viral 2C and 3A proteins, which promotes the assembly of the replication complexes, as well as cellular poly(A) binding protein (PABP). Coimmunoprecipitation assays confirmed that these proteins are complexed with RHA. We have also identified a novel interaction between RHA and the S fragment in the FMDV 5′ nontranslated region. Moreover, a reduction in the expression of RHA, using RHA-specific small interfering RNA constructs, inhibited FMDV replication. These results indicate that RHA plays an essential role in the replication of FMDV and potentially other picornaviruses through ribonucleoprotein complex formation at the 5′ end of the genome and by interactions with 2C, 3A, and PABP.

Foot-and-mouth disease virus (FMDV) is a highly contagious viral pathogen of cloven-hoofed animals (22). Infection can occur through direct contact with infected animals or indirectly by aerosol transmission, with symptoms appearing 2 to 3 days postexposure. Outbreaks of FMDV among livestock of disease-free nations have had extremely deleterious effects on the economies of those countries, since international trade of animals and animal products from countries experiencing an FMD outbreak is strictly forbidden (22, 34, 48). Indeed, several economically devastating outbreaks have occurred over the past decade on almost every continent. A chemically inactivated whole-virus vaccine has been used to contain the disease, but it is slow acting and does not permit distinction between infected and vaccinated animals (7, 8, 21, 40).

FMDV is a prototypic member of the *Aphthovirus* genus of the family *Picornaviridae* (15, 39). The infectious virion is a nonenveloped icosahedron composed of four structural proteins (VP1 to VP4), which surrounds a positive-sense single-stranded RNA genome. The genome encodes a single open reading frame, which is translated into a large polyprotein that is subsequently cleaved to produce 14 mature virus proteins by three virus proteases (L^{pro}, $2A^{pro}$, and $3C^{pro}$) (9). The virus translation products include the four structural proteins and 10 nonstructural proteins (NSPs) (L^{pro}, $2A^{pro}$, 2B, 2C, 3A, $3B_1$ to $3B_3$, $3C^{pro}$, and $3D^{pol}$). During viral replication, the genomic RNA not only directs the synthesis of the viral polyprotein but also serves as template for RNA synthesis. Studies of other picornaviruses including poliovirus have revealed that the processes of translation and RNA replication cannot occur simultaneously on the same RNA molecule (42, 55–57). Therefore, a molecular switch must exist that shuts down translation, thus allowing for the initiation of RNA replication. It has been demonstrated in the context of flaviviruses that the circularization of the single-stranded positive-sense RNA genome through an interaction of the 5′ and 3′ nontranslated regions (NTRs) halts translation and allows for initiation of RNA replication (1–3, 31, 54). In the case of poliovirus, the bridge between the NTRs appears to be mediated by interactions of cellular and virus factors bound to the respective NTRs, specifically the virus-encoded 3CD precursor and the cellular poly(C) binding protein (PCBP2) and poly(A) binding protein (PABP) (4, 19). Recently, the 5′ and 3′ NTRs of FMDV were shown to physically interact in vitro in the absence of cellular or viral protein. When mixed with cellular extracts, different portions of the NTRs coprecipitated four different proteins migrating at 120, 70, 45, and 30/34 kDa (49). The identities of p45 and p70 were confirmed to be PCBP2 and PABP, respectively. However, the identity and role in the virus life cycle of the p120 and p30/34 proteins remain unknown.

RNA helicase A (RHA) with an approximate molecular mass of 130 kDa was first reported to unwind double-stranded DNA and was later found to have higher affinity for double-stranded RNA (59–62). RHA, also known as DHX9 and NDHII, possesses two double-stranded RNA binding domains at the N terminus, with a classical DEAD box/helicase domain in the center, and the extreme C terminus possesses arginine-glycine-glycine (RGG) repeats (59). RHA shuttles back and

* Corresponding author. Mailing address: Plum Island Animal Disease Center, USDA/ARS/NAA, P.O. Box 848. Greenport, NY 11944-0848. Phone: (631) 323-3177. Fax: (631) 323-3006. E-mail: elizabeth.rieder@ars.usda.gov.

† Supplemental material for this article may be found at http://jvi.asm.org/.

▽ Published ahead of print on 26 August 2009.

forth between the nucleus and the cytoplasm but maintains steady-state levels in the nucleus (6, 18). The nuclear transport domain is localized at the C terminus, where asymmetric dimethylation of arginine residues in the C-terminal RGG repeats has been reported to promote the nuclear retention of RHA (50). In addition to helicase activity, RHA exhibits diverse functions in the cell, most notably the enhancement of gene expression by bridging CBP/p300 with RNA polymerase II (5). Recent studies have shown an RHA-specific enhancement of gene expression in response to alpha interferon (IFN) (16), and RHA binding to the p65 subunit of nuclear factor kappa B (NF-κB) resulted in increased NF-κB-stimulated gene expression (53); both findings implicate RHA involvement in the innate immune response.

In addition to its established cellular functions, RHA has been implicated in the replication cycles of several viruses including retroviruses, flaviviruses, and adenoviruses (11, 25, 28–30, 35, 36, 47). In the case of human immunodeficiency virus (HIV), RHA increased transcription of the HIV genome through specific binding to stem-loop structures known as transcriptional activating regions (35, 44). Overexpression of RHA has been found to increase HIV transcription rates severalfold. Additionally, RHA exhibits activity similar to that of the HIV Rev protein, facilitating the nuclear export of unspliced viral transcripts. Type D retroviruses, which do not encode a Rev-like viral factor, rely upon cellular RHA exclusively for nuclear export of their unspliced RNA transcripts (17). Although until now RHA has never been examined in the context of picornaviruses, it has been described as a bridging factor between the 5′ and 3′ NTRs of flaviviruses, leading to circularization of the positive-sense single-stranded genome (28). Potentially, FMDV may utilize host cell RHA in a similar manner, ceasing viral translation and triggering RNA synthesis.

In this report, we demonstrate that infection with FMDV stimulates a subcellular reorganization of RHA from the nucleus to the cytoplasm of infected cells, which is coincident with an increase in the cellular levels of nonmethylated RHA. The alteration in the subcellular distribution of RHA did not require the action of the virus leader protease. The cytoplasmic RHA was found in close proximity to some FMDV NSPs and some cellular factors. Moreover, RHA coprecipitated with FMDV 2C and 3A as well as cellular PABP. It was also found to bind the S fragment from the FMDV 5′ NTR in vitro, suggesting that it may interact with the virus genome in the infected host cell. RHA appears to be an essential cellular factor in the replication of the virus genome, evidenced from the significant reduction in virus titer observed when RHA is knocked down with RHA-specific small interfering RNAs (siRNAs).

MATERIALS AND METHODS

Materials. N^6-Methyl-2′-deoxyadenosine (MDA), DL-homocysteine, adenosine, and the in vitro XTT [2,3,bis(2-methoxy-4-nitro-5-sulfophenyl)-2H-tetrazolium-5-carboxanilide] based toxicology assay kit (Tox-2) were purchased from Sigma-Aldrich (Saint Louis, MO). Mirus siQUEST siRNA transfection reagent was purchased from Mirus Bio Corporation (Madison, WI). SuperSignal West Dura chemiluminescent substrate and Seize X protein G-coupled beads were purchased from Pierce Biotechnology (Rockford, IL).

Viruses, cells, and plasmid construction. FMDV types A_{12} and A_{24} Cruzeiro/Brazil 1955 (A_{24} Cruzeiro, GenBank accession no. AY593768) were derived from the infectious cDNA clones pRMC35 and pA_{24}Cru (45, 46). Isolates of FMDV O1 Campos (GenBank accession no. AJ320488), C3 Resende, and SAT2 viruses and bovine enterovirus 1 (BEV-1; GenBank accession no. D00214) were obtained from Marvin Grubman or Peter Mason, Agricultural Research Service, Plum Island. A_{24} Cruzeiro carrying a deletion of the leader coding sequence (LL) was produced by site-directed mutagenesis of full-length genome copy plasmid pA_{24}Cru to produce LL-pA_{24}Cru. The baby hamster kidney strain 21, clone 13 cell line (BHK-21) was maintained in Eagle's basal medium (Life Technologies, Gaithersburg, MD) supplemented with 10% bovine calf serum (HyClone, South Logan, UT), 10% tryptose phosphate broth, and antibiotic-antimycotic. The LFBK cell line was cultured in 10% fetal bovine serum in Dulbecco's minimal essential medium supplemented with antibiotic-antimycotic (51). Cells were grown at 37°C in a humidified 5% CO_2 atmosphere. Expression plasmids pET26b-Ub/$3C^{pro}$ and pET26b-Ub/$3D^{pol}$ encoding type A FMDV $3C^{pro}$ and $3D^{pol}$ sequences were amplified by PCR primers 5′-GCGGAATTCCCGCGGTGGAAGTGGTGCCCCACCGACC-3′ (plus-strand sequence) and 5′-GCGGAATTCGGATCCCTCGTGTTGTGGTTCAGGGTC-3′ (minus-strand sequence) and primers 5′-GCGGAATTCCCGCGGTGGAGGGTTAATCGTTGATAC-3′ (plus-strand sequence) and 5′-GCGGAATTCGGATCCTGCGTCACCGCACACGGCGTTCACCC-3′ (minus-strand sequence), respectively. The fragments were digested with SacII and BamHI and then ligated into the same sites of pET26b-Ub to produce pET26b-Ub/$3C^{pro}$ (kindly provided by Craig E. Cameron) (20). Glutathione *S*-transferase (GST)–RHA1 was kindly provided by Toshi Nakajima (5).

Antibodies. Rabbit polyclonal anti-RHA was purchased from Bethyl Laboratories (Montgomery, TX). Mouse monoclonal anti-RHA (later designated anti-DM-RHA) and mouse monoclonal anti-PABP were purchased from Abcam (Cambridge, MA). Mouse monoclonal anti-PCBP2 was purchased from Abnova (Walnut, CA). Vivian O'Donnell and Marvin Grubman generously provided rabbit polyclonal anti-FMDV 3A and anti-FMDV 2C, respectively. Alfonso Clavijo (National Centre for Foreign Animal Diseases, Canada) generously provided mouse monoclonal anti-FMDV $3D^{pol}$. Goat anti-rabbit antibodies conjugated with Alexa Fluor 488 (AF488; green) and goat anti-mouse antibodies conjugated with Alexa Fluor 568 (AF568; red) were purchased from Molecular Probes (Eugene, OR). Goat anti-rabbit and goat anti-mouse antibodies conjugated with horseradish peroxidase (HRP) were purchased from Sigma-Aldrich (Saint Louis, MO).

Immunofluorescent microscopy (IFM). LFBK cells were seeded on glass coverslips in 12-well plates and grown to approximately 50% confluence. Uninfected control cells were immediately fixed with 4% paraformaldehyde (PF) in phosphate-buffered saline (PBS) prior to the introduction of virus into adjacent wells. After fixation of the control cells, the remaining wells containing cells on coverslips were infected with FMDV A_{24} Cruzeiro wild type (WT) at a multiplicity of infection (MOI) of 10 and incubated at 37°C for 1 h. Afterwards, excess virus was removed by acid washing the cells briefly, followed by several rinses with virus growth medium (VGM) consisting of Eagle's basal medium supplemented with 100 mM L-glutamine and antibiotic-antimycotic. Designated cells were then fixed with 4% PF for 1 h postinfection (hpi). The remaining cells were provided with fresh VGM; incubated for 2, 3, 4, 5, or 6 hpi at 37°C; and then fixed with 4% PF. Cells were washed in PBS, permeabilized with 0.1% Triton X-100 in PBS, and blocked with 3% bovine serum albumin with 10 mM glycine. Then, cells were probed with the indicated primary antibodies followed by secondary antibodies conjugated with AF488 (green) or AF568 (red) with three consecutive PBS washes after each antibody treatment. The coverslips were then air dried and mounted onto glass slides with ProLong antifade medium supplemented with DAPI (4′,6-diamidino-2-phenylindole) nuclear stain (Molecular Probes). Cells were examined, and images were captured using 40× and 100× objectives on an Olympus fluorescent microscope. Images were refined, and figures were generated using Adobe Photoshop software (Adobe Systems, San Jose, CA).

Coimmunoprecipitation. Following the manufacturer's protocol, antibodies directed against cellular PCBP2 and PABP as well as FMDV 2C, 3A, $3C^{pro}$, and $3D^{pol}$ were separately bound to the Seize X protein G agarose beads (Pierce). Both LFBK and BHK-21 cells infected with FMDV or uninfected were lysed with 0.5% Nonidet P-40 in PBS supplemented with protease inhibitors and benzonase (Novagen, Gibbstown, NJ). Subsequently, uninfected or virus-infected cell lysates were individually mixed with the different sets of antibody-coupled beads, washed, and eluted. Bound protein was eluted using a low-pH solution (pH 2.5) provided by the Seize X immunoprecipitation kit (Pierce) and was immediately thereafter neutralized with 1 M Tris, pH 8. For each immunoprecipitation reaction, the flowthrough, three pooled washes, and three eluates were collected. Samples were mixed with Laemmli sample buffer (33), boiled, and analyzed by Western blot probing with anti-RHA (Bethyl Laboratories).

Western blotting. Sodium dodecyl sulfate-polyacrylamide gel electrophoresis was carried out using a 12% Nu-PAGE precast gel system (Invitrogen, Carlsbad,

CA). Subsequently, the separated proteins were electroblotted onto a nitrocellulose membrane (Sigma). After being blocked with 5% milk in PBS-Tween, specific proteins were detected with primary antibodies followed by goat anti-rabbit or goat anti-mouse antibodies conjugated with HRP (Sigma). Cellular tubulin, employed as an internal loading control protein, was detected with an HRP-conjugated monoclonal antibody (Tubulin-α AB-2; Lab Vision, Fremont, CA). The bound HRP conjugate antibodies were reacted with the WestDura SuperSignal chemiluminescent reagent (Pierce) according to the manufacturer's instructions and visualized on X-ray film (X-Omat; Kodak, Rochester, NY).

RNA filter binding assay. Viral cDNA corresponding to the sense S fragment, the 3′ NTR, and *cis*-acting *r*eplication *e*lements (*cre*) (38) of the FMDV genome was amplified from plasmid $pA_{24}Cru$ (see above) by using standard PCR with specific oligonucleotides containing the T7 promoter at the 5′ end of the sense oligonucleotide. Various concentrations of purified proteins from eluates corresponding to endogenous RHA coimmunoprecipitated with FMDV 2C and 3A proteins were separately mixed with positive-sense fragment RNAs labeled with [^{32}P]CTP in binding buffer (5 mM morpholinepropanesulfonic acid [MOPS], 25 mM KCl, 2 mM $MgCl_2$, 5 mM dithiothreitol). After being mixed at room temperature for 15 min in the presence of an excess of nonspecific RNA (15 μg tRNA), the protein-RNA complexes were applied to prewetted nitrocellulose membranes (0.45-μm pore size; Sigma) overlying a nylon membrane (Hybond-N$^+$; Amersham) as described previously (58). Filters were washed twice with buffer (20 mM HEPES-KOH [pH 6.8], 1 mM magnesium acetate, 5 mM 2-mercaptoethanol) and dried, and the radioactive products were detected by Kodak X-Omat films. Protein concentration of RHA in the eluates was determined using both Western blot analysis and silver staining of 12% sodium dodecyl sulfate-polyacrylamide gels (Invitrogen).

RNA interference. Four siRNA constructs targeted to different regions of the RHA gene designated RHA-6, RHA-9, RHA-10, and RHA-11 were purchased from Qiagen (Valencia, CA). Additionally, two nonsense siRNA negative-control constructs were purchased from Dharmacon and designated Dh-1 and Dh-3 (Lafayette, CO). The four RHA-specific siRNA constructs and the negative-control siRNA constructs were transfected into LFBK cells using Mirus siQUEST siRNA transfection reagent (Mirus Bio Corporation). The four RHA siRNAs were transfected in combination after assay development showed the most effective reduction in endogenous RHA by this method. Briefly, the RHA-targeted siRNA constructs and the nonsense siRNA controls were diluted to a concentration of 50 nM in serum-free Dulbecco's minimal essential medium (Invitrogen) and siQUEST (Mirus Bio Corporation). Cells grown to 60 to 70% confluence were incubated at 37°C with the specified siRNA dilutions for 72 h. Cells were harvested by being scraped into solution, and the subsequent lysates were evaluated for a reduction in RHA protein concentration by Western blot probing with anti-RHA (Bethyl Laboratories) and subsequently with antitubulin-HRP (Lab Vision) as a loading control. The relative concentrations of RHA and tubulin after each siRNA treatment were evaluated by ImageJ software (available at http://rsb.info.nih.gov/ij; developed by Wayne Rasband, National Institutes of Health, Bethesda, MD), and the extrapolated values were plotted using Microsoft Excel (Redmond, WA). Cell viability after siRNA treatment was determined by XTT assay (Sigma) following the manufacturer's protocol and by counting trypan blue-excluding cells with a Neubauer hemacytometer.

Viral growth, virus yield inhibition, and plaque assays. To assess the effects of the siRNA treatments on virus replication in LFBK cells, monolayers transfected with siRNA cocktails as described above were infected with the specified virus at an MOI of 10^{-3} PFU/cell (unless otherwise indicated). Following virus absorption for 1 h, the inoculum was removed and VGM was added to the cells. After 24 h at 37°C, virus-infected cells were harvested and viral titers were determined by plaque assay as previously described (45). Plates were fixed and stained with crystal violet (0.3% in Histochoice; Amresco, Solon, OH), and the plaques were counted. The values calculated for the number of PFU per milliliter were plotted in a logarithmic scale using Microsoft Excel (Microsoft). All assays were performed in triplicate.

RESULTS

FMDV infection alters RHA subcellular localization. RHA has been reported to shuttle between the nucleus and the cytoplasm, while maintaining a steady-state concentration in the nucleus (6, 18, 50). In the context of other RNA viruses, infection has previously been shown to trigger the accumulation of RHA in the cytoplasm (28). To determine if the nuclear localization of RHA can be altered as a result of FMDV infection, the distributions of RHA in uninfected and FMDV-infected LFBK cells were compared. LFBK cells were infected with FMDV A_{24} Cruzeiro and examined at different stages of infection by IFM as described in Materials and Methods. As shown in Fig. 1A and the bottom of Fig. 1B, RHA was concentrated in the nucleus of uninfected LFBK cells as well as in FMDV-infected cells examined at approximately 1 hpi. In contrast, as FMDV infection progressed from 2 to 6 hpi, infected cells demonstrated increased RHA-specific cytoplasmic fluorescence in the form of RHA-specific fluorescent puncta. The same effect was observed for other strains of FMDV including A12, O1 Campos, C3 Resende, and SAT2 (data not shown). For the remainder of the experiments, the A_{24} Cruzeiro strain was used unless otherwise specified.

To determine if this effect was unique to FMDV or could be reflective of other picornaviruses, we looked for a change in the subcellular distribution of RHA in LFBK cells infected with BEV-1. As shown in the top panels of Fig. 1B, the accumulation of RHA in the cytoplasm was detected much earlier in LFBK cells infected with BEV-1 than in those infected with A_{24} Cruzeiro (Fig. 1B, bottom). By 5 hpi, RHA was completely cytoplasmic in greater than 95% of the cells observed on the BEV-1 slides. The complete redistribution of RHA from the nucleus to the cytoplasm was infrequently observed in FMDV-infected cells. These results suggested that RHA redistribution to the cytoplasm might be a phenomenon of other picornaviruses and not just FMDV. Additionally, these findings demonstrated that the degree to which the subcellular localization of RHA is altered during infection varies depending on the picornavirus being examined.

Nonmethylated RHA accumulates with infection. It has previously been reported that nuclear retention of RHA is favored when arginine residues in its C-terminal RGG motifs are methylated through the action of the PRMT1 arginine methyltransferase (50). To evaluate the methylation state of the RHA accumulated in the cytoplasm following FMDV infection, we obtained a mouse monoclonal antibody that recognizes only nonmethylated RHA, hereafter referred to as DM-RHA. LFBK cells infected with FMDV were examined at different time points by IFM using anti-DM-RHA (Fig. 2A, upper panels) and the rabbit polyclonal anti-RHA previously used (Fig. 2A, lower panels). DM-RHA was below the detection limit in uninfected LFBK cells, while the first RHA-specific fluorescence was not detected until 3 hpi. The nonmethylated RHA was observed mostly in the cytoplasm, though some puncta were observed in the nucleus. Contrastingly, the rabbit polyclonal anti-RHA detected nuclear RHA fluorescence in the uninfected samples and was able to detect cytoplasmic fluorescent puncta that appear to be RHA specific earlier than the anti-DM-RHA at 2 hpi (Fig. 2A). At 3 to 4 hpi, the intensities and amounts of cytoplasmic fluorescence observed were comparable for the two antibodies.

To confirm that inhibition of arginine methylation would result in the accumulation of RHA in the cytoplasm in the absence of infection and to reinforce the idea that the anti-DM-RHA antibody specifically recognized DM-RHA, we examined infected and uninfected LFBK cells cultured in media supplemented with compounds that promote the accumulation of a potent methylation inhibitor, MDA. As shown in Fig. 2B, uninfected cells cultured with the methylation inhibitor cock-

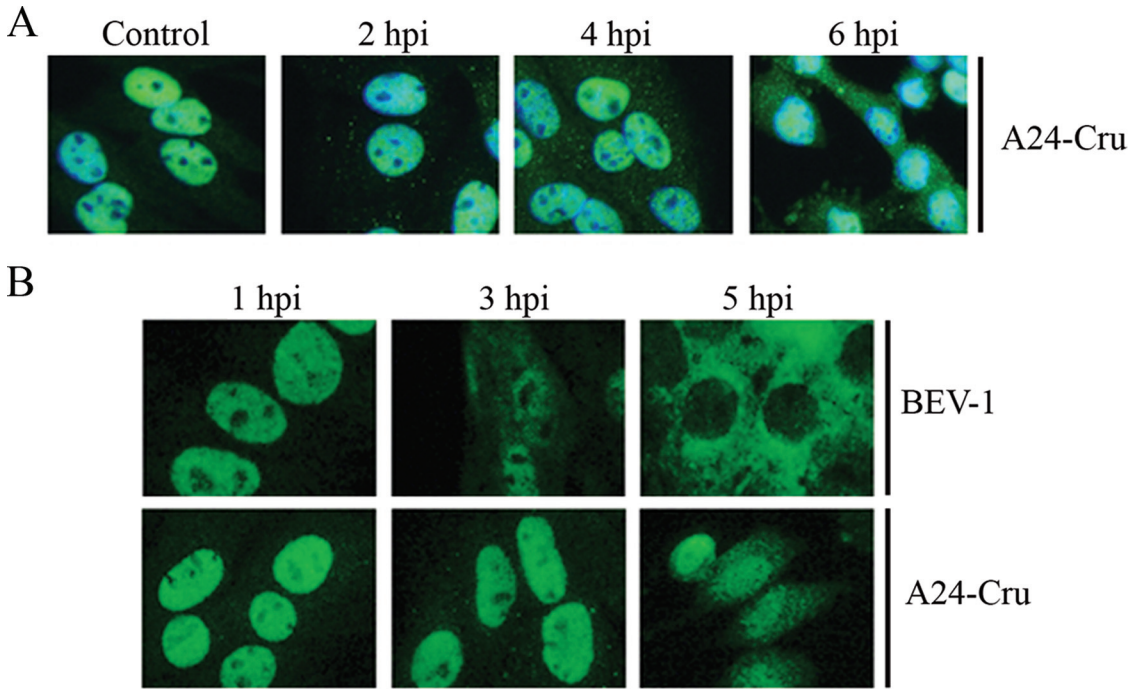

FIG. 1. FMDV infection alters RHA subcellular localization. (A) Uninfected and FMDV-infected (A_{24} Cruzeiro) LFBK cells were probed with rabbit anti-RHA followed by goat anti-rabbit–AF488 (green) with nuclear material being stained with DAPI (blue). Samples included uninfected control cells and infected cells at 2, 4, and 6 hpi. (B) LFBK cells infected with BEV-1 (top) or FMDV A_{24} Cruzeiro (bottom) at 1, 3, and 5 hpi were probed with rabbit anti-RHA, followed by goat anti-rabbit–AF488 (green); DAPI staining is not shown.

tail showed cytoplasmic DM-RHA-specific fluorescence comparable to what was previously observed for FMDV-infected LFBK cells at 3 to 4 hpi in the absence of methylation inhibitors. Similarly, cells infected with FMDV with or without the MDA treatment exhibited large amounts of cytoplasmic DM-RHA at all time points examined (Fig. 2B). We concluded that the anti-DM-RHA antibody specifically reacted with nonmethylated RHA and that the alteration in RHA localization during FMDV infection is coincident with a change in its methylation state. Additionally, the prior inhibition of methylation resulting in RHA redistribution to the cytoplasm did not impair subsequent FMDV infection given that the production of one of the virus NSPs, 3A, was unaffected by incubation in the presence of the MDA cocktail. The immunofluorescence data were corroborated by Western blot analysis of virus-infected and uninfected cell lysates, where infection was conducted in the presence of 0, 0.1, 0.5, and 1 mM MDA. As shown in Fig. 2C, the quantities of viral 3A, $3C^{pro}$, and $3D^{pol}$ produced during FMDV infection were unaffected by the MDA inhibitor cocktail except at 1 mM MDA, where there was a detectable reduction in viral protein synthesis.

We also wanted to determine if the prior inhibition of RHA methylation might benefit FMDV infection. LFBK cells preincubated with the MDA cocktail at 0, 0.1, 0.5, and 1 mM were infected with FMDV at an MOI of 10^{-3} for 24 h at 37°C. Harvested samples were serially diluted and applied to confluent monolayers of BHK-21 cells to determine the resulting virus titer. As shown in Fig. 2D, incubation with 0.1 and 0.5 mM MDA slightly enhanced the virus titer. Consistent with the Western blotting data in Fig. 2C, higher concentrations of MDA (1 mM and greater) appeared to be cytotoxic, which was confirmed by trypan blue exclusion staining (data not shown). Thus, we surmised that the accumulation of nonmethylated RHA in the cytoplasm provided some benefit to the progression of FMDV infection.

FMDV leader proteinase does not trigger RHA redistribution. In the context of the closely related cardioviruses, the virus leader protein has been shown to trigger the redistribution of certain host proteins from the nucleus (37). Although functionally distinct from the cardiovirus leader protein, FMDV possesses a leader protein, L^{pro}, which is a viral protease known to enter the nucleus during infection. Upon entry to the nucleus, FMDV L^{pro} has been reported to antagonize the innate immune response via degradation of the p65/RelA subunit of NF-κB. To investigate the possibility that FMDV leader protein was responsible for the redistribution of RHA from the nucleus, we examined the RHA localization in cells infected with A_{24} Cruzeiro WT relative to cells infected with a "leaderless" A24 FMDV mutant (LL) derived from plasmid LL-pA_{24}Cru (see Materials and Methods for details) (Fig. 3).

To this end, infected and uninfected cells were examined at different time points by IFM, simultaneously probing with anti-DM-RHA and antibodies directed against L^{pro}. L^{pro}-specific fluorescence was detected at 3 hpi in cells infected with the WT FMDV (Fig. 3). As expected, cells infected with the "leaderless" FMDV mutant failed to exhibit L^{pro}-specific fluorescence at any of the time points tested. Consistent with earlier results, DM-RHA was first detected in cells infected with the WT FMDV at approximately 3 hpi (Fig. 3). Identical results were obtained with cells infected with the "leaderless" FMDV, con-

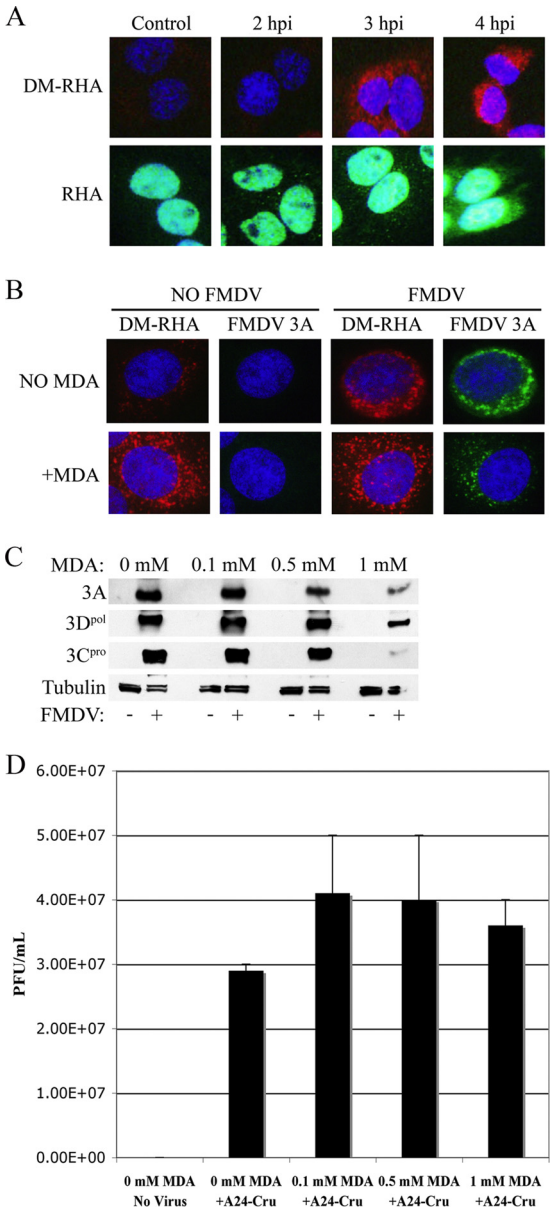

FIG. 2. Nonmethylated RHA accumulates with infection. (A) Uninfected and FMDV-infected LFBK cells were probed with rabbit anti-RHA (designated RHA) followed by goat anti-rabbit–AF488 (green). Alternatively, the samples were probed with a mouse RHA antibody that recognizes only the demethylated form of RHA (designated DM-RHA) followed by goat anti-mouse–AF568 (red). Nuclear material was stained with DAPI (blue). (B) LFBK cells were or were not pretreated with the MDA cocktail and infected or not infected with FMDV in the continued presence or absence of MDA. Infected cells were examined at 4 hpi. Samples were then probed with mouse anti-DM-RHA followed by goat anti-mouse–AF568 (red) and with rabbit anti-3A followed by goat anti-rabbit–AF488 (green). Nuclear material was stained with DAPI (blue). (C) LFBK cells were treated with 0, 0.1, 0.5, and 1 mM MDA cocktail and then infected or not with FMDV in the continued presence or absence of MDA. Cellular lysates were prepared from harvested uninfected and infected cells and were examined by Western blot probing with antibodies to FMDV 3A, $3C^{pro}$, $3D^{pol}$, and tubulin. (D) The samples harvested in panel C were also examined by plaque assay (see Materials and Methods). The counted plaques were used to calculate the virus titer, and the values were plotted onto a bar graph using Microsoft Excel.

firming that L^{pro} is not responsible for the change in RHA distribution from the nucleus to the cytoplasm in FMDV-infected cells.

RHA redistributes to the same cytoplasmic region where FMDV replication processes occur. Next, we carried out experiments to determine if the RHA-specific fluorescence observed in the cytoplasm in FMDV-infected cells was in proximity to virus NSPs, particularly those associated with virus replication. As such, FMDV-infected and uninfected LFBK cells were examined by IFM simultaneously probing with anti-RHA and antibodies specific to individual NSPs that participate in viral RNA replication, specifically 2C, 3A, and RNA polymerase $3D^{pol}$. FMDV 2C, 3A, and $3D^{pol}$ were detected by IFM no earlier than 2 to 3 hpi. 2C, 3A, and $3D^{pol}$ were first observed in a punctate perinuclear pattern at 3 to 4 hpi, and some fluorescent puncta were detected for $3D^{pol}$, but not 2C and 3A, within the nucleus (Fig. 4A, B, and C). As previously observed, RHA accumulation in the cytoplasm was detected at approximately 3 to 4 hpi (Fig. 4). The RHA-specific fluorescence demonstrated some overlap with both 2C- and 3A-associated fluorescence (Fig. 4A and B) but seldom with $3D^{pol}$ (Fig. 4C). This observed overlap suggested the possibility that RHA may be a host cell factor recruited to the cytoplasm concomitantly with increasing expression of the viral proteins 2C and 3A, to assist with specific viral processes.

We also sought to determine if RHA localized in the cytoplasm proximal to PCBP2 and/or PABP, which has previously been demonstrated to interact with portions of the FMDV genome and the genome of other picornaviruses during RNA replication (26, 49). A comparison of uninfected and FMDV-infected cells by IFM revealed that PCBP2 was predominantly nuclear with some perinuclear cytoplasmic fluorescence in uninfected cells (Fig. 4D). However, at 4 hpi, PCBP2 was largely confined to the cytoplasm with little to no nuclear fluorescence. The change in subcellular distribution of PCBP2 was mirrored by RHA. Unlike PCBP2, PABP was exclusively cytoplasmic in all cell lines tested whether infected or uninfected (Fig. 4E). Although the distribution of PABP in the cytoplasm was not altered during FMDV infection, the diffuse PABP-specific fluorescence coalesced into discrete puncta at 4 hpi. Overlap of the PABP-specific puncta with RHA-specific cytoplasmic puncta in FMDV-infected cells was also observed (Fig. 4E). These observations allowed us to conclude that as a result of FMDV infection, RHA relocalizes to the cytoplasm in close proximity to cellular and viral proteins involved in the viral replication complex.

RHA interacts with FMDV 2C and 3A and cellular PABP. Given the possible overlap of RHA-specific fluorescent puncta with those of FMDV 2C and 3A, we carried out coimmunoprecipitation experiments to determine if the overlap in fluorescence corresponded to an actual interaction, whether direct or indirect. We also wanted to examine the possibility that RHA interacted with other NSPs with which it did not colocalize, such as $3C^{pro}$ and $3D^{pol}$. To this end, lysates of both LFBK and BHK-21 (not shown) cells collected at different stages of infection with FMDV were prepared using a lysis buffer that contained a nuclease (see Materials and Methods) to ensure that any interaction detected was truly protein-protein and not mediated by nucleic acid. Lysates of cells infected with FMDV at an MOI of 10 were immunoprecipitated with

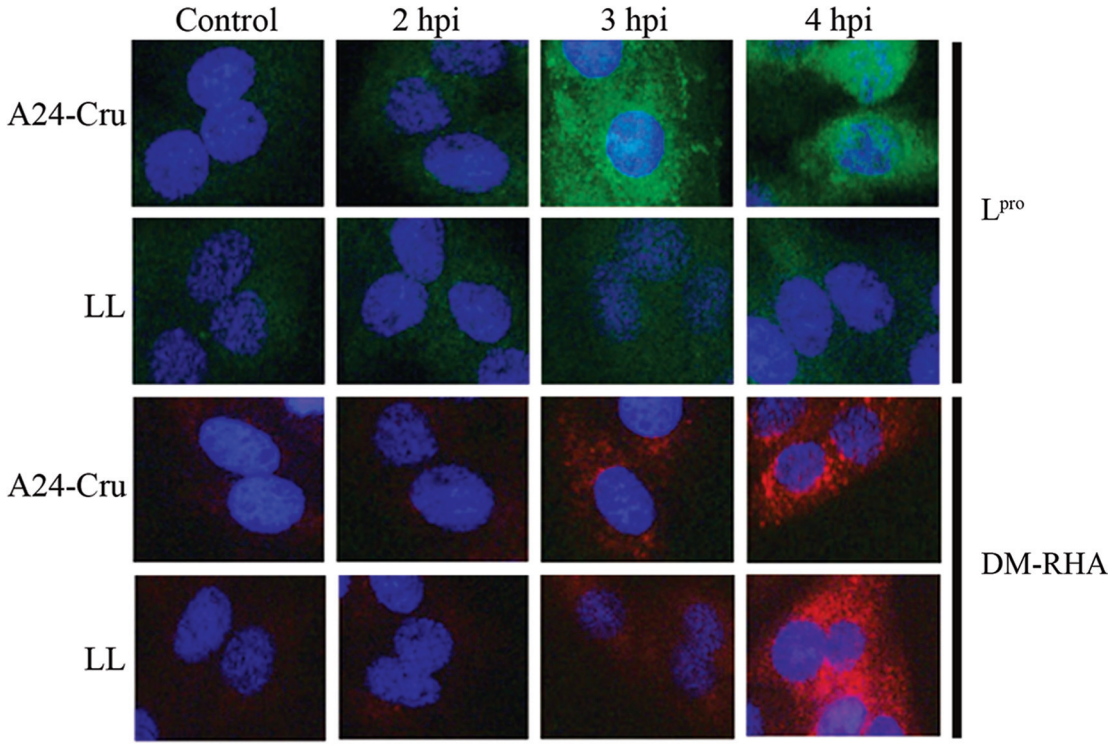

FIG. 3. RHA redistribution is not triggered by FMDV leader proteinase (L^{pro}). LFBK cells were infected with either the WT A_{24} Cruzeiro strain of FMDV or a "leaderless" derivative (LL) lacking the coding region for L^{pro}. Uninfected and infected cells were probed simultaneously with rabbit anti-L^{pro} (indicated panels) and mouse anti-DM-RHA (indicated panels) followed by goat anti-rabbit–AF488 (green) and goat anti-mouse–AF568 (red).

Seize X protein G beads coupled with antibodies directed against FMDV 2C, 3A, $3C^{pro}$, and $3D^{pol}$ separately. Eluates collected for each time point during infection were examined by Western blot probing with anti-RHA. A single band migrating at the approximate molecular weight of RHA was first detected in FMDV-infected cell lysates immunoprecipitated with anti-2C and anti-3A as early as 2 hpi and was observed at each successive time point (3 to 4 hpi shown in Fig. 5). In strong contrast, beads coupled to anti-$3C^{pro}$ and anti-$3D^{pol}$ antibodies separately repeatedly failed to precipitate RHA at any of the time points tested (Fig. 5). Similarly, 24-h time points of lysates of cells infected with FMDV at an MOI of 10^{-3} showed RHA coprecipitating with FMDV 2C and 3A. These results were consistent with the IFM data showing RHA-2C and RHA-3A overlap. Moreover, the lack of detection of RHA-$3D^{pol}$ overlap by IFM was consistent with the failure to coprecipitate RHA with $3C^{pro}$ and $3D^{pol}$. These results indicated that during the course of FMDV infection, RHA interacts with viral 2C and 3A, further suggesting that RHA was situated on the membranous structures generated by 2C and 3A in the host cell. Furthermore, given that FMDV 2C and 3A do not enter the host cell nucleus, the precipitated RHA represents a cytoplasmic pool of the protein that has been relocalized from the nucleus.

Given the data from the IFM experiments, we also investigated if RHA coprecipitated with cellular proteins PCBP2 and PABP. Immunoprecipitation reactions were conducted with Seize X protein G beads coupled with anti-PCBP2 and anti-PABP separately. Despite the overlap of fluorescence observed in Fig. 4D, coimmunoprecipitation experiments using anti-PCBP2 antibodies failed to precipitate RHA at any time point tested, including samples incubated for 24 h and infected at an MOI of 10^{-3} (Fig. 5). In contrast, immunoprecipitation reactions using anti-PABP coprecipitated RHA as early as 4 hpi as shown in Fig. 5. RHA interaction with PABP became more prominent at 24 hpi from lysates infected at an MOI of 10^{-3}.

RHA interacts with the S fragment of the FMDV 5′ NTR. To explore the potential interaction of RHA with replication elements contained in the FMDV NTRs, single-stranded RNA corresponding to the positive-sense orientation of the S fragment, the *cis*-acting replication element (*cre*), and the 3′ NTR were produced and labeled with ^{32}P. Initially, we tested mixtures of RHA copurified with FMDV 2C or 3A, which were mixed in binding buffer with the ^{32}P-labeled RNA probes, and the potential resulting complexes were analyzed by filter binding assays as described in Materials and Methods. As shown in Fig. 6A, autoradiography showed that with increasing concentrations RHA-2C or RHA-3A retained ^{32}P-labeled S fragment in a dose-dependent fashion. We also examined the eluates from immunoprecipitation reactions with anti-$3C^{pro}$ and anti-$3D^{pol}$, which did not coprecipitate RHA (Fig. 5). Interestingly, we observed that eluates from the anti-$3C^{pro}$ group were capable of binding to the S fragment in the presence of an excess of tRNA (data not shown and Fig. 6C). In contrast, the $3D^{pol}$

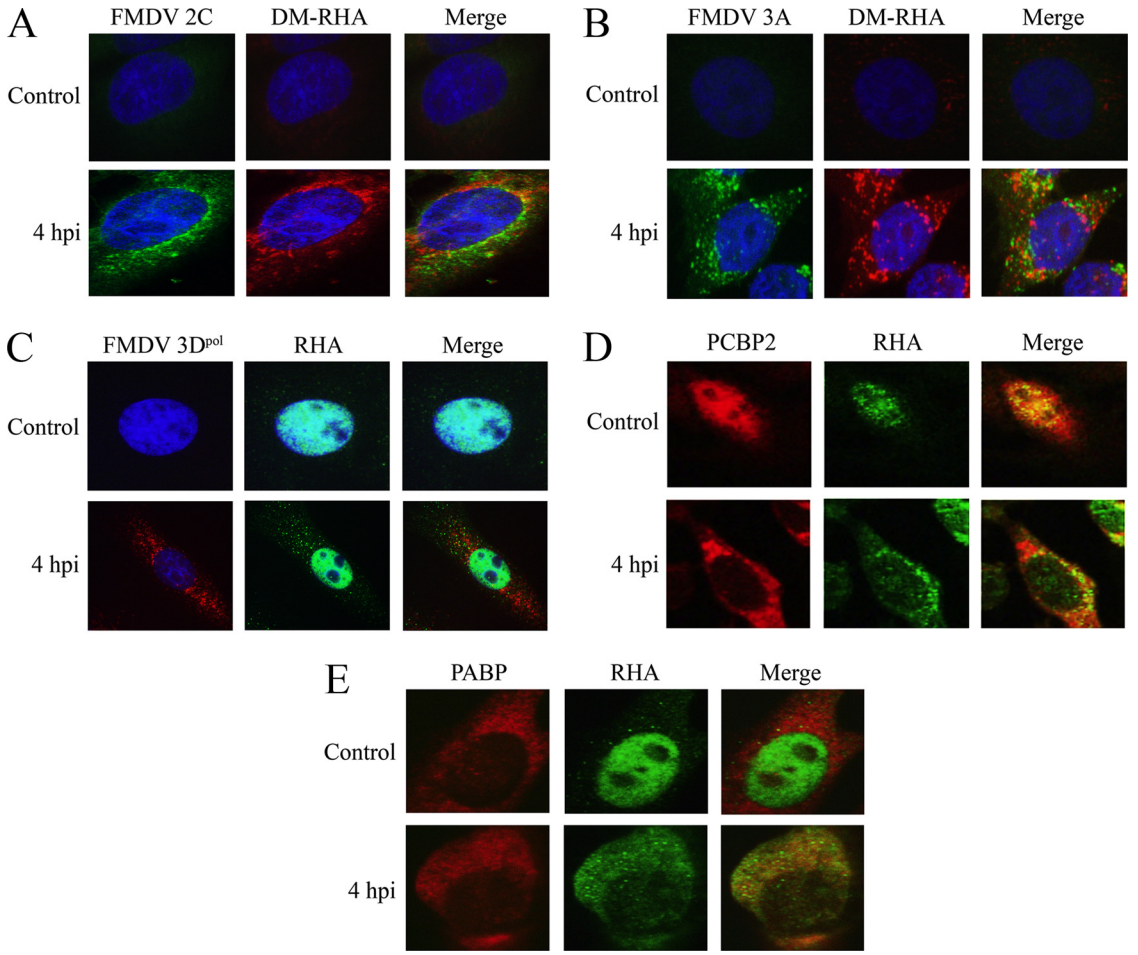

FIG. 4. Cytoplasmic RHA overlaps with viral and cellular components of the FMDV replication complex. Uninfected and FMDV-infected LFBK cells at 4 hpi were simultaneously probed with mouse anti-DM-RHA and rabbit anti-2C (A), mouse anti-DM-RHA and rabbit anti-3A (B), rabbit anti-RHA and mouse anti-3D^{pol} (C), rabbit anti-RHA and mouse anti-PCBP2 (D), or rabbit anti-RHA and mouse anti-PABP (E) followed by goat anti-rabbit–AF488 (green) and goat anti-mouse–AF568 (red). Nuclear material was stained with DAPI (blue) (A to E).

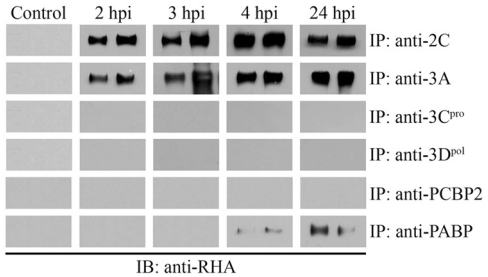

FIG. 5. RHA coprecipitates with FMDV 2C and 3A and cellular PABP. Uninfected LFBK cells or cells infected with FMDV at an MOI of 10 were harvested at 2, 3, and 4 hpi, and cells infected with FMDV at an MOI of 10^{-3} were harvested at 24 hpi. Lysates were immunoprecipitated with anti-PCBP2-, anti-PABP-, anti-2C-, anti-3A-, anti-3C^{pro}-, and anti-3D^{pol}-coupled agarose beads (Seize X protein G beads). Bound protein was eluted using a low-pH solution (pH 2.5), and the collected samples were analyzed by Western blot probing with anti-RHA. For each immunoprecipitation reaction, two consecutive eluates are represented in the figure for each time point examined.

eluates did not show any specific affinity for ^{32}P-labeled S fragment (data not shown and Fig. 6C).

Given that the RNA binding experiments described above used mixtures of proteins, we next wanted to evaluate the specific contribution of RHA to the binding of the S fragment. Additionally, given that the low-pH elution may have disrupted the protein structure, we wanted to strengthen the prior results using an alternative source of RHA. To that end, we obtained a GST-tagged purified fragment of RHA, specifically the N-terminal first 250 amino acids of RHA known to include two double-stranded RNA binding domains and designated RHA1 (5). This protein was tested for its ability to bind the ^{32}P-labeled S fragment, *cre*, and 3′ NTR probes. As shown in Fig. 6B, binding of the RHA1 subunit was confirmed for the S-fragment RNA probe but not when using the *cre* or 3′ NTR RNA probes. Similarly, we wanted to reinforce the idea that 3C^{pro} was directly responsible for the observation that the anti-3C^{pro} eluates specifically bound the S fragment (Fig. 6A). Full-length 3C^{pro} and 3D^{pol} were expressed and purified from bacteria and examined for their ability to interact with ^{32}P-labeled S fragment as described elsewhere (see Materials and Methods). The full-length 3C^{pro} specifically bound the S frag-

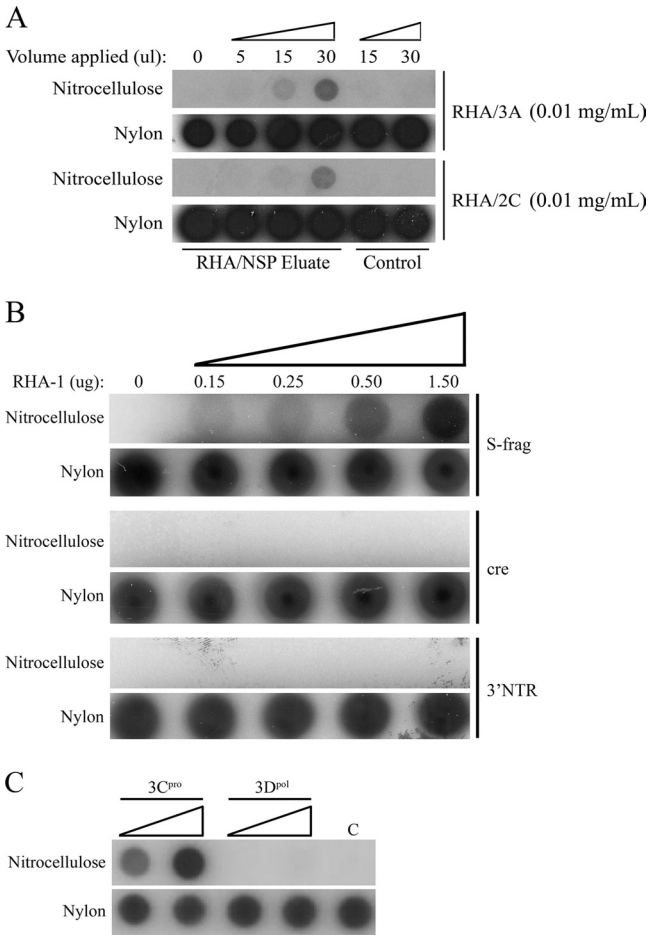

FIG. 6. RHA interacts with the S fragment of the FMDV 5′ NTR. (A) Eluates from the immunoprecipitation reactions described in the legend to Fig. 5 were mixed with ^{32}P-labeled positive-sense single-stranded RNA corresponding to the FMDV S fragment. Samples were tested for protein-RNA interaction using the filter binding assay (see Materials and Methods). (B) Purified RHA1 was mixed separately with ^{32}P-labeled S fragment, *cre*, and 3′ NTR and evaluated for protein-RNA interaction as described for panel A. (C) Purified 3C^{pro} and 3D^{pol} were separately mixed with ^{32}P-labeled S fragment and evaluated for protein-RNA interaction as described for panel A.

ment in the presence of a large excess of tRNA (Fig. 6C). As was observed with the anti-3D^{pol} eluates, the purified 3D^{pol} did not interact with S fragment (Fig. 6C). Together, these results showed that RHA and 3C^{pro} specifically bind the FMDV S fragment. Future studies will focus on the determination of the contact point for the interaction between RHA and the S fragment.

Knockdown of RHA expression reduces FMDV titer. To test for the importance of RHA in the life cycle of FMDV, four siRNA molecules targeted to different regions of the RHA gene (numbered 6, 9, 10, and 11) were employed. LFBK cells were transfected with one, two, or four of the RHA-targeted siRNA constructs or two nonsense siRNA negative controls and incubated at 37°C for 72 h. Exposure to RHA-targeted siRNAs did not impact cell viability relative to that of untransfected cells and cells transfected with negative-control siRNAs as determined by the XTT assay (Fig. 7C; see also Fig. S1 in the supplemental material) and trypan blue exclusion staining (data not shown). The cells were then infected or not with FMDV at an MOI of 10^{-3} for 24 h at 37°C. Subsequently, the samples were harvested and the resulting cell lysates were analyzed by Western blot probing with anti-RHA and antitubulin (loading control). The siRNA constructs targeted to the RHA gene demonstrated mixed efficacy in reducing the concentration of endogenous RHA, with the tandem transfection of all four RHA-specific siRNA constructs being the most effective at reducing the cellular concentration of RHA (Fig. 7A and B; see also Fig. S1 in the supplemental material). The nonsense siRNA molecules had no effect on RHA concentration, mirroring untransfected controls (Fig. 7A and B; see also Fig. S1 in the supplemental material). All subsequent experiments used the four RHA-specific siRNA constructs in combination.

Next, we wanted to evaluate the effect of a reduction in RHA expression on the progress of FMDV infection. The blot in Fig. 7A was also probed with anti-3D^{pol} to determine if the reduction in RHA affected the production of a virus NSP. Prior incubation with the four RHA-specific siRNA constructs negatively impacted 3D^{pol} production such that it was undetectable on Western blots relative to untransfected cells and cells transfected with negative-control siRNAs (Fig. 7A and B). The RHA knockdown by siRNA was repeated, and each harvested sample was serially diluted and applied to confluent monolayers of BHK-21 cells for virus titration. The transfection of the four siRNA molecules for RHA reduced the number of PFU by approximately 3 logs relative to cells transfected with nonsense siRNA constructs (Fig. 7D). Use of one or two RHA siRNAs was not as effective at reducing FMDV titer as was using the four siRNAs in combination (data not shown). These results led us to the conclusion that RHA plays a vital role in the life cycle of FMDV, evidenced from the strong effect that perturbations in RHA expression had on virus titer. Identical results were obtained when this experiment was repeated using BEV-1 (data not shown), indicating that RHA is potentially a vital factor in the life cycle of some other picornaviruses.

DISCUSSION

Viruses are dependent on the host cell for their replication and as such modify a variety of cellular signal transduction pathways. To counter some of the host immune responses, viruses have developed very sophisticated mechanisms to subvert the host defense and to recruit protein factors from the cellular machinery to support their own replication. Considerable progress has been made in understanding the critical roles that viral and cell proteins play in determining virus tropism, infectivity, and disease development. In this study, we reported that the cellular RHA protein is involved in the life cycle of FMDV. Indeed, through IFM and coimmunoprecipitation methods, we determined that the subcellular distribution of RHA dramatically shifts from the nucleus to the cytoplasm during the course of FMDV infection, where it interacts with components of the virus replication complex. Remarkably, we have shown that a reduction in the concentration of endogenous RHA negatively impacted the progression of FMDV infection. These results were mirrored in several different strains of FMDV as well as in an unrelated picornavirus,

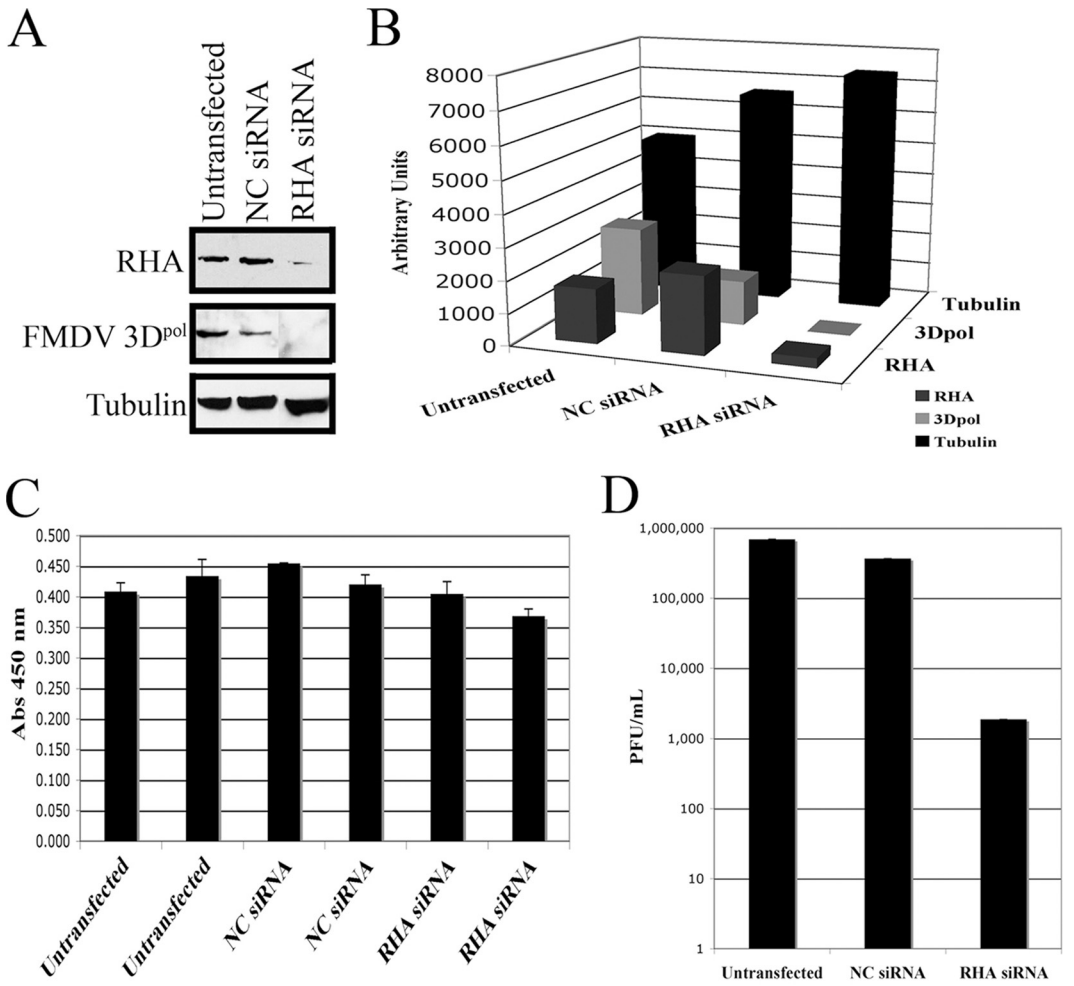

FIG. 7. Knockdown of RHA expression reduces FMDV titer. LFBK cells were transfected and incubated with or without nonspecific siRNA constructs or constructs directed against RHA for 72 h and infected with FMDV. (A) The concentration of endogenous RHA and virus $3D^{pol}$ in each sample was evaluated by Western blot probing with anti-RHA and anti-$3D^{pol}$. The blot was also probed with antitubulin to confirm equal loading between lanes. (B) The Western blot from panel A was scanned, and the relative intensity of the detected bands was quantified using the ImageJ software. Quantities determined for each indicated protein were plotted side by side in a bar graph using Microsoft Excel. (C) Prior to virus infection, cells transfected or not with the various siRNA constructs were evaluated for cytotoxicity using the XTT assay. The absorbances obtained at 450 nm were plotted using Microsoft Excel. Two independent experiments are shown for each condition. (D) Samples were serially diluted and applied to confluent monolayers of BHK-21 cells for a virus titer assay. Calculated virus titers were plotted in logarithmic scale using Microsoft Excel. NC, negative control.

BEV-1, implying that this is a critical factor in the replication of members of the *Aphthovirus* and *Enterovirus* genera of the *Picornaviridae*. To the best of our knowledge, this study demonstrated for the first time the involvement of RHA in the life cycle of any picornavirus.

The alteration in RHA appearance from nuclear to punctate cytoplasmic in FMDV-infected cells resembles the phenomena reported for cells infected with the flaviviruses hepatitis C virus and bovine viral diarrhea virus (28). In particular, in cells containing replicating hepatitis C virus RNA, it was shown that the generally nuclear NF/NFAR proteins, which include RHA, accumulate in cytoplasmic viral replication complexes.

We then asked whether RHA relocalization to the cytoplasm in FMDV-infected cells is due to alteration of the nuclear export pathway or the result of changes in the RHA protein itself via alterations in the nuclear localization signal located at the C terminus. Consistent with published data, our results showed that inhibition of CRM-1, which is implicated in the export of proteins and transport of many mRNAs from the nucleus (27, 52), did not have any deleterious effect on RHA redistribution (data not shown). Nuclear retention of RHA has been attributed to methylation of RGG motifs present in the extreme C terminus of the protein (50). Indeed, treatment of cell cultures with a methylation inhibitor cocktail in the absence of virus produced a similar accumulation of RHA in the cytoplasm (Fig. 2). Moreover, using an antibody specific for the nonmethylated form of RHA (DM-RHA), we confirmed that the RHA that accumulated in the cytoplasm during FMDV infection is nonmethylated. Given the temporal accumulation of nonmethylated RHA in the cytoplasm observed upon infection, it is tempting to suggest that the virus may have triggered the demethylation of RHA. Interestingly, true arginine de-

methylases have only recently been discovered (12, 32). It will be interesting to investigate whether FMDV and other picornaviruses interact with this new family of enzymes, revealing a previously unreported significance of protein methylation in virus infection.

Virus-induced redistribution of nuclear proteins has been attributed to a variety of virus-encoded proteases. In the case of poliovirus, the 2A protease ($2A^{pro}$) was demonstrated to cleave critical components of the nuclear pore complex, which resulted in the accumulation of host nuclear proteins such as nucleolin, hnRNP K, and Sam68 in the cytoplasm (23, 24). Nonproteolytic viral proteins such as the L protein of cardioviruses also induce changes in the normal nucleocytoplasmic transport patterns (37). While FMDV does not possess the functional equivalent of the poliovirus $2A^{pro}$, it does encode a leader proteinase (L^{pro}), which has been reported to shut down host cell translation through cleavage of eIF4GI and also antagonizes the innate immune response through degradation of the NF-κB p65 subunit (13). While the redistribution of RHA observed during infection with BEV-1 (which does not possess the FMDV L^{pro}) implied that this protein is not involved, we wished to conclusively evaluate its relative importance to the observed RHA redistribution during FMDV infection. Using a "leaderless" mutant strain of A_{24} Cruzeiro FMDV, we were able to rule out the involvement of L^{pro} in the virus-induced redistribution of RHA. For polioviruses, the viral proteinase $3C^{pro}$ is utilized to cleave the host protein PCBP2, which has been implicated in the shutdown of viral translation and initiation of replication of the virus genome (4, 19, 43). The FMDV $3C^{pro}$, on the other hand, has been shown to cleave several cellular translation initiation factors such as eIF4A and eIF4G (10). While $3C^{pro}$ proteolysis of the nuclear transport domain of RHA is an attractive mechanism to explain the alteration in RHA distribution during viral infection, we did not detect RHA cleavage in FMDV-infected samples. Furthermore, we were unable to coprecipitate RHA with $3C^{pro}$ antibodies, indicating that these two proteins do not interact.

The significance of the recruitment of RHA to the cytoplasm is likely twofold: enhancement of virus-specific processes and countering of certain cellular defense mechanisms induced following viral entry into the cells. In this regard, two recent publications described a role for RHA in the innate immune response of the cell (16, 53). In one example, RHA was found to interact with the p65 subunit of NF-κB, which resulted in enhanced expression of NF-κB expressed genes (53). Similarly, it was shown that, when stimulated by alpha IFN, RHA migrated to promyelocytic leukemia nuclear bodies, where it assists in the enhancement of expression of IFN-stimulated genes (16). Therefore, by removing RHA away from the nucleus, FMDV is likely to complement the activity of the L^{pro} in effectively inhibiting the cellular innate immune response (13, 14). This strategy does not seem to be unique to RNA viruses; for instance, adenoviruses produce virus-associated RNA II which specifically binds and sequesters RHA to the cytoplasm (36). However, removing RHA from the nucleus to prevent its enhancement of the innate immune response cannot be the only benefit to the virus, given that the protein associates with two of the virus NSPs as well as with the highly structured 5′ end of the virus genome.

Cytoplasmic RHA was shown to be in close proximity to and to interact with FMDV NSPs involved with virus replication, 2C and 3A. Additionally, RHA interacted with PABP. Given the established roles of cellular PABP and FMDV 2C and 3A in RNA replication, these findings indicate the potential participation of RHA in the processes performed by these proteins. This contention is further supported by the demonstration that RHA interacts with the positive-sense strand of the S fragment at the extreme 5′ terminus of the FMDV genome in consistency with a model in which the 5′-terminal S fragment and the 3′ NTR of FMDV RNA interact via RNA-RNA interaction (49) and ribonucleoprotein complex formation (this study) to mediate and regulate translation and replication. In this regard, a recent study has shown that DHX9 RNA helicase interacts with the hepatitis C virus and FMDV internal ribosome entry site elements; however, the significance of these interactions remains to be elucidated (41). Additionally, another publication by the same authors suggested that RHA does not significantly affect the function of the FMDV internal ribosome entry site, which is consistent with our own preliminary data (P. Lawrence, E. Rieder, and E. Martinez-Salas, unpublished results). We speculate that the recruitment of RHA to the cytoplasm could also potentially assist in the unwinding of double-stranded RNA intermediates during the replication of the virus genome either by itself or in association with the viral protein 2C.

Our findings provided evidence that upon FMDV infection a nonmethylated form of RHA is redistributed to the cytoplasm where interacting partners of the viral replication complexes (viral RNA and NSPs) localize. Since RHA depletion inhibited viral infection, the identification of the specific sequence motif required for the formation of RNA-protein and protein-protein complexes could be of value in the understanding of the mechanism of RHA function and in the design of new antiviral drugs targeting these complexes.

ACKNOWLEDGMENTS

We thank Lisa Aschenbrenner for expert assistance in this study, Craig E. Cameron for the pET26b-Ub expression plasmid, Toshi Nakajima for the GST-RHA1 expression plasmid, and Aniko Paul for providing RHA1 purified protein.

REFERENCES

1. **Alvarez, D. E., C. V. Filomatori, and A. V. Gamarnik.** 2008. Functional analysis of dengue virus cyclization sequences located at the 5′ and 3′UTRs. Virology **375:**223–235.
2. **Alvarez, D. E., M. F. Lodeiro, C. V. Filomatori, S. Fucito, J. A. Mondotte, and A. V. Gamarnik.** 2006. Structural and functional analysis of dengue virus RNA. Novartis Found. Symp. **277:**120–132.
3. **Alvarez, D. E., M. F. Lodeiro, S. J. Luduena, L. I. Pietrasanta, and A. V. Gamarnik.** 2005. Long-range RNA-RNA interactions circularize the dengue virus genome. J. Virol. **79:**6631–6643.
4. **Andino, R., N. Boddeker, D. Silvera, and A. V. Gamarnik.** 1999. Intracellular determinants of picornavirus replication. Trends Microbiol. **7:**76–82.
5. **Aratani, S., R. Fujii, T. Oishi, H. Fujita, T. Amano, T. Ohshima, M. Hagiwara, A. Fukamizu, and T. Nakajima.** 2001. Dual roles of RNA helicase A in CREB-dependent transcription. Mol. Cell. Biol. **21:**4460–4469.
6. **Aratani, S., T. Oishi, H. Fujita, M. Nakazawa, R. Fujii, N. Imamoto, Y. Yoneda, A. Fukamizu, and T. Nakajima.** 2006. The nuclear import of RNA helicase A is mediated by importin-alpha3. Biochem. Biophys. Res. Commun. **340:**125–133.
7. **Balamurugan, V., R. M. Kumar, and V. V. Suryanarayana.** 2004. Past and present vaccine development strategies for the control of foot-and-mouth disease. Acta Virol. **48:**201–214.
8. **Beard, C., G. Ward, E. Rieder, J. Chinsangaram, M. J. Grubman, and P. W. Mason.** 1999. Development of DNA vaccines for foot-and-mouth disease, evaluation of vaccines encoding replicating and non-replicating nucleic acids in swine. J. Biotechnol. **73:**243–249.

9. **Belsham, G. J.** 2005. Translation and replication of FMDV RNA. Curr. Top. Microbiol. Immunol. **288:**43–70.
10. **Belsham, G. J., G. M. McInerney, and N. Ross-Smith.** 2000. Foot-and-mouth disease virus 3C protease induces cleavage of translation initiation factors eIF4A and eIF4G within infected cells. J. Virol. **74:**272–280.
11. **Bolinger, C., A. Yilmaz, T. R. Hartman, M. B. Kovacic, S. Fernandez, J. Ye, M. Forget, P. L. Green, and K. Boris-Lawrie.** 2007. RNA helicase A interacts with divergent lymphotropic retroviruses and promotes translation of human T-cell leukemia virus type 1. Nucleic Acids Res. **35:**2629–2642.
12. **Chang, B., Y. Chen, Y. Zhao, and R. K. Bruick.** 2007. JMJD6 is a histone arginine demethylase. Science **318:**444–447.
13. **de Los Santos, T., S. de Avila Botton, R. Weiblen, and M. J. Grubman.** 2006. The leader proteinase of foot-and-mouth disease virus inhibits the induction of beta interferon mRNA and blocks the host innate immune response. J. Virol. **80:**1906–1914.
14. **de Los Santos, T., F. Diaz-San Segundo, and M. J. Grubman.** 2007. Degradation of nuclear factor kappa B during foot-and-mouth disease virus infection. J. Virol. **81:**12803–12815.
15. **Domingo, E., E. Baranowski, C. Escarmis, and F. Sobrino.** 2002. Foot-and-mouth disease virus. Comp. Immunol. Microbiol. Infect. Dis. **25:**297–308.
16. **Fuchsova, B., P. Novak, J. Kafkova, and P. Hozak.** 2002. Nuclear DNA helicase II is recruited to IFN-alpha-activated transcription sites at PML nuclear bodies. J. Cell Biol. **158:**463–473.
17. **Fujii, R., M. Okamoto, S. Aratani, T. Oishi, T. Ohshima, K. Taira, M. Baba, A. Fukamizu, and T. Nakajima.** 2001. A role of RNA helicase A in cis-acting transactivation response element-mediated transcriptional regulation of human immunodeficiency virus type 1. J. Biol. Chem. **276:**5445–5451.
18. **Fujita, H., T. Ohshima, T. Oishi, S. Aratani, R. Fujii, A. Fukamizu, and T. Nakajima.** 2005. Relevance of nuclear localization and functions of RNA helicase A. Int. J. Mol. Med. **15:**555–560.
19. **Gamarnik, A. V., and R. Andino.** 2000. Interactions of viral protein 3CD and poly(rC) binding protein with the 5′ untranslated region of the poliovirus genome. J. Virol. **74:**2219–2226.
20. **Gohara, D. W., C. S. Ha, S. Kumar, B. Ghosh, J. J. Arnold, T. J. Wisniewski, and C. E. Cameron.** 1999. Production of "authentic" poliovirus RNA-dependent RNA polymerase (3D(pol)) by ubiquitin-protease-mediated cleavage in Escherichia coli. Protein Expr. Purif. **17:**128–138.
21. **Grubman, M. J.** 2005. Development of novel strategies to control foot-and-mouth disease: marker vaccines and antivirals. Biologicals **33:**227–234.
22. **Grubman, M. J., and B. Baxt.** 2004. Foot-and-mouth disease. Clin. Microbiol. Rev. **17:**465–493.
23. **Gustin, K. E.** 2003. Inhibition of nucleo-cytoplasmic trafficking by RNA viruses: targeting the nuclear pore complex. Virus Res. **95:**35–44.
24. **Gustin, K. E., and P. Sarnow.** 2001. Effects of poliovirus infection on nucleo-cytoplasmic trafficking and nuclear pore complex composition. EMBO J. **20:**240–249.
25. **He, Q. S., H. Tang, J. Zhang, K. Truong, F. Wong-Staal, and D. Zhou.** 2008. Comparisons of RNAi approaches for validation of human RNA helicase A as an essential factor in hepatitis C virus replication. J. Virol. Methods **154:**216–219.
26. **Herold, J., and R. Andino.** 2001. Poliovirus RNA replication requires genome circularization through a protein-protein bridge. Mol. Cell **7:**581–591.
27. **Hutten, S., and R. H. Kehlenbach.** 2007. CRM1-mediated nuclear export: to the pore and beyond. Trends Cell Biol. **17:**193–201.
28. **Isken, O., M. Baroth, C. W. Grassmann, S. Weinlich, D. H. Ostareck, A. Ostareck-Lederer, and S. E. Behrens.** 2007. Nuclear factors are involved in hepatitis C virus RNA replication. RNA **13:**1675–1692.
29. **Isken, O., C. W. Grassmann, R. T. Sarisky, M. Kann, S. Zhang, F. Grosse, P. N. Kao, and S. E. Behrens.** 2003. Members of the NF90/NFAR protein group are involved in the life cycle of a positive-strand RNA virus. EMBO J. **22:**5655–5665.
30. **Jeang, K. T., and V. Yedavalli.** 2006. Role of RNA helicases in HIV-1 replication. Nucleic Acids Res. **34:**4198–4205.
31. **Khromykh, A. A., H. Meka, K. J. Guyatt, and E. G. Westaway.** 2001. Essential role of cyclization sequences in flavivirus RNA replication. J. Virol. **75:**6719–6728.
32. **Klose, R. J., and Y. Zhang.** 2007. Regulation of histone methylation by demethylimination and demethylation. Nat. Rev. Mol. Cell Biol. **8:**307–318.
33. **Laemmli, U. K.** 1970. Cleavage of structural proteins during the assembly of the head of bacteriophage T4. Nature **227:**680–685.
34. **Leforban, Y., G. Gerbier, and M. Rweyemamu.** 2002. Action of FAO in the control of foot and mouth disease. Comp. Immunol. Microbiol. Infect. Dis. **25:**373–382.
35. **Li, J., H. Tang, T. M. Mullen, C. Westberg, T. R. Reddy, D. W. Rose, and F. Wong-Staal.** 1999. A role for RNA helicase A in post-transcriptional regulation of HIV type 1. Proc. Natl. Acad. Sci. USA **96:**709–714.
36. **Liao, H. J., R. Kobayashi, and M. B. Mathews.** 1998. Activities of adenovirus virus-associated RNAs: purification and characterization of RNA binding proteins. Proc. Natl. Acad. Sci. USA **95:**8514–8519.
37. **Lidsky, P. V., S. Hato, M. V. Bardina, A. G. Aminev, A. C. Palmenberg, E. V. Sheval, V. Y. Polyakov, F. J. van Kuppeveld, and V. I. Agol.** 2006. Nucleocytoplasmic traffic disorder induced by cardioviruses. J. Virol. **80:**2705–2717.
38. **Mason, P. W., S. V. Bezborodova, and T. M. Henry.** 2002. Identification and characterization of a *cis*-acting replication element (*cre*) adjacent to the internal ribosome entry site of foot-and-mouth disease virus. J. Virol. **76:**9686–9694.
39. **Mason, P. W., M. J. Grubman, and B. Baxt.** 2003. Molecular basis of pathogenesis of FMDV. Virus Res. **91:**9–32.
40. **McKenna, T. S., E. Rieder, J. Lubroth, T. Burrage, B. Baxt, and P. W. Mason.** 1996. Strategy for producing new foot-and-mouth disease vaccines that display complex epitopes. J. Biotechnol. **44:**83–89.
41. **Pacheco, A., S. Reigadas, and E. Martinez-Salas.** 2008. Riboproteomic analysis of polypeptides interacting with the internal ribosome-entry site element of foot-and-mouth disease viral RNA. Proteomics **8:**4782–4790.
42. **Paul, A. V., C. F. Yang, S. K. Jang, R. J. Kuhn, H. Tada, M. Nicklin, H. G. Krausslich, C. K. Lee, and E. Wimmer.** 1987. Molecular events leading to poliovirus genome replication. Cold Spring Harbor Symp. Quant. Biol. **52:**343–352.
43. **Perera, R., S. Daijogo, B. L. Walter, J. H. Nguyen, and B. L. Semler.** 2007. Cellular protein modification by poliovirus: the two faces of poly(rC)-binding protein. J. Virol. **81:**8919–8932.
44. **Reddy, T. R., H. Tang, W. Xu, and F. Wong-Staal.** 2000. Sam68, RNA helicase A and Tap cooperate in the post-transcriptional regulation of human immunodeficiency virus and type D retroviral mRNA. Oncogene **19:**3570–3575.
45. **Rieder, E., T. Bunch, F. Brown, and P. W. Mason.** 1993. Genetically engineered foot-and-mouth disease viruses with poly(C) tracts of two nucleotides are virulent in mice. J. Virol. **67:**5139–5145.
46. **Rieder, E., T. Henry, H. Duque, and B. Baxt.** 2005. Analysis of a foot-and-mouth disease virus type A24 isolate containing an SGD receptor recognition site in vitro and its pathogenesis in cattle. J. Virol. **79:**12989–12998.
47. **Roy, B. B., J. Hu, X. Guo, R. S. Russell, F. Guo, L. Kleiman, and C. Liang.** 2006. Association of RNA helicase a with human immunodeficiency virus type 1 particles. J. Biol. Chem. **281:**12625–12635.
48. **Rweyemamu, M. M., and V. M. Astudillo.** 2002. Global perspective for foot and mouth disease control. Rev. Sci. Technol. **21:**765–773.
49. **Serrano, P., M. R. Pulido, M. Saiz, and E. Martinez-Salas.** 2006. The 3′ end of the foot-and-mouth disease virus genome establishes two distinct long-range RNA-RNA interactions with the 5′ end region. J. Gen. Virol. **87:**3013–3022.
50. **Smith, W. A., B. T. Schurter, F. Wong-Staal, and M. David.** 2004. Arginine methylation of RNA helicase a determines its subcellular localization. J. Biol. Chem. **279:**22795–22798.
51. **Swaney, L. M.** 1988. A continuous bovine kidney cell line for routine assays of foot-and-mouth disease virus. Vet. Microbiol. **18:**1–14.
52. **Tang, H., D. McDonald, T. Middlesworth, T. J. Hope, and F. Wong-Staal.** 1999. The carboxyl terminus of RNA helicase A contains a bidirectional nuclear transport domain. Mol. Cell. Biol. **19:**3540–3550.
53. **Tetsuka, T., H. Uranishi, T. Sanda, K. Asamitsu, J. P. Yang, F. Wong-Staal, and T. Okamoto.** 2004. RNA helicase A interacts with nuclear factor kappaB p65 and functions as a transcriptional coactivator. Eur. J. Biochem. **271:**3741–3751.
54. **Villordo, S. M., and A. V. Gamarnik.** 2009. Genome cyclization as strategy for flavivirus RNA replication. Virus Res. **139:**230–239.
55. **Wimmer, E., C. U. Hellen, and X. Cao.** 1993. Genetics of poliovirus. Annu. Rev. Genet. **27:**353–436.
56. **Wimmer, E., R. J. Kuhn, S. Pincus, C. F. Yang, H. Toyoda, M. J. Nicklin, and N. Takeda.** 1987. Molecular events leading to picornavirus genome replication. J. Cell Sci. Suppl. **7:**251–276.
57. **Wimmer, E., and A. Nomoto.** 1993. Molecular biology and cell-free synthesis of poliovirus. Biologicals **21:**349–356.
58. **Yin, J., A. V. Paul, E. Wimmer, and E. Rieder.** 2003. Functional dissection of a poliovirus *cis*-acting replication element [PV-*cre*(2C)]: analysis of single- and dual-*cre* viral genomes and proteins that bind specifically to PV-*cre* RNA. J. Virol. **77:**5152–5166.
59. **Zhang, S., and F. Grosse.** 1997. Domain structure of human nuclear DNA helicase II (RNA helicase A). J. Biol. Chem. **272:**11487–11494.
60. **Zhang, S., and F. Grosse.** 2004. Multiple functions of nuclear DNA helicase II (RNA helicase A) in nucleic acid metabolism. Acta Biochim. Biophys. Sin. (Shanghai) **36:**177–183.
61. **Zhang, S., C. Herrmann, and F. Grosse.** 1999. Pre-mRNA and mRNA binding of human nuclear DNA helicase II (RNA helicase A). J. Cell Sci. **112:**1055–1064.
62. **Zhou, K., K. T. Choe, Z. Zaidi, Q. Wang, M. B. Mathews, and C. G. Lee.** 2003. RNA helicase A interacts with dsDNA and topoisomerase IIalpha. Nucleic Acids Res. **31:**2253–2260.